Structural Evolution of the Binary System Ba-Si under High-pressure and High-temperature Conditions

Shoji Yamanaka and Shoichi Maekawa

Department of Applied Chemistry, Graduate School of Engineering, Hiroshima University, Higashi-Hiroshima 739-8527, Japan

Reprint requests to Prof. S. Yamanaka. E-mail: syamana@hiroshima-u.ac.jp

Z. Naturforsch. **61b,** 1493 – 1499 (2006); received June 19, 2006

A new silicon-rich binary compound $BaSi_6$ has been prepared by the treatment of the Ba_8Si_{46} clathrate compound under a pressure of 15 GPa at 1000 °C, or from a stoichiometric mixture of $BaSi_2$ and Si by treatment under similar high-pressure and high-temperature conditions. The Rietveld refinements revealed that $BaSi_6$ is isomorphous with $EuGa_2Ge_4$, and crystallizes with space group *Cmcm* and the lattice parameters $a = 4.485(1)$, $b = 10.375(2)$, and $c = 11.969(3)$ Å. Each Ba atom is surrounded by 18 Si atoms in an irregularly shaped polyhedron $@Si_{18}$. The polyhedra are connected by sharing faces to form Ba containing tunnels along the *a* axis. All of the Si-rich compounds so far with atomic ratios Si/Ba > 2 in the binary system have been prepared only under high-pressure and high-temperature conditions. There is a general tendency that the Si/Ba ratio of the compounds increases with an increase of the pressure in the preparation.

Key words: Ba-Si System, $BaSi_6$, High-pressure Phase, Clathrate

Introduction

The binary compound $BaSi_2$ containing $[Si_4]^{4-}$ Zintl anions crystallizes in an orthorhombic structure [1], which is stable on compression up to 7.1 GPa at r. t. At elevated temperatures, however, it undergoes an orthorhombic-trigonal transition at 5.2 GPa and 400 °C, and a trigonal-cubic transition at 600 °C [2, 3]. The structures found in the Ba-Si binary system are shown in Fig. 1. The high-pressure phases with the trigonal and cubic structures have the $EuGe_2$ (or $CaSi_2$-like) and the $SrSi_2$ structures, respectively, which correspond to the structures of other disilicides of alkaline earth metals with smaller atomic radii [3, 4]. Binary compounds with atomic ratios Si/Ba > 2 can be obtained only under high pressures at elevated temperatures. $Ba_{24}Si_{100}$ (Si/Ba $= 4.17$) was prepared under a pressure of 1.5 GPa at 800 °C [5] and Ba_8Si_{46} (Si/Ba $= 5.75$) under a pressure of 3.0 GPa at 800 °C [6]. When $Ba_{24}Si_{100}$ is compressed under a pressure of 3 GPa at 800 °C, it decomposes into a mixture of Ba_8Si_{46} and Ba. These silicon-rich binary compounds belong to a silicon clathrate family: Ba_8Si_{46} is isotypic with Type I gas (G) hydrate $G_x(H_2O)_{46}$ [7]. The H–O···H hydrogen bonds of the gas hydrates are replaced by the Si-Si covalent bonds in the Si clathrate compound, and Ba atoms are trapped in silicon polyhedral cages, two dodecahedra ($@Si_{20}$: 5^{12}) and six tetrakaidecahedra ($@Si_{24}$: $5^{12}6^2$) in the unit cell. The two types of polyhedra are linked by face sharing to form the A15 or β-tungsten structure. Ba_8Si_{46} is a superconductor with a critical temperature (T_c) of 8.0 K. Note that this is the first superconductor composed of a Si-sp^3 three-dimensional network. $Ba_{24}Si_{100}$ also consists of Ba containing silicon dodecahedral cages ($Ba@Si_{20}$), which are linked by sharing pentagonal faces to form a chiral zeolite-like network; the rest of the Ba atoms are located in the interstices of the network. Recently, it has been found that $Ba_{24}Si_{100}$ can also become a superconductor at $T_c = 1.4$ K [8].

San-Miguel *et al.* [9] studied the structural change of Ba_8Si_{46} under high pressure using a diamond anvil cell (DAC) at r. t. They revealed that Ba_8Si_{46} was homothetically compressed up to 30 GPa with a reduction of the volume by 25%, and reversibly recovered on releasing the pressure. At higher pressures, above 40 GPa, irreducible amorphization occurred. An excellent review on the high-pressure properties of group IV clathrates was given by San-Miguel and Toulemonde [10]. In this study, the structural change of Ba_8Si_{46} under high-pressure conditions at elevated

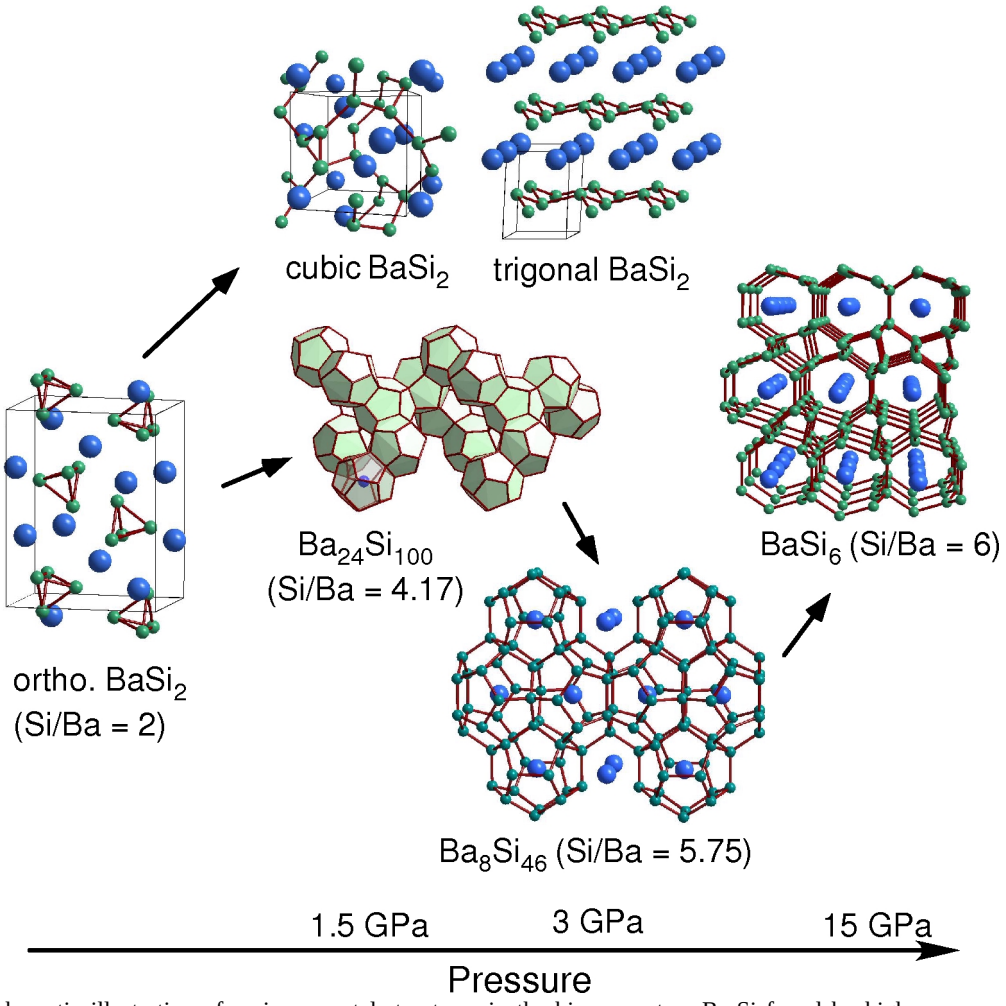

Fig. 1. Schematic illustration of various crystal structures in the binary system Ba-Si found by high-pressure and high-temperature treatments; orthorhombic $BaSi_2$ is transformed to trigonal $BaSi_2$ and cubic $BaSi_2$.

temperatures has been investigated, and a new Si-rich clathrate-like phase with a composition of $BaSi_6$ has been found.

Results and Discussion

A new binary compound was obtained by the treatment of Ba_8Si_{46} under a pressure of 15 GPa at 1000 °C. The XRD powder pattern could be indexed on the basis of an orthorhombic unit cell with $a = 4.485(1)$, $b = 10.375(2)$, and $c = 11.969(3)$ Å. The composition was determined to be $BaSi_{5.99}$ (Ba: 45.6, Si: 55.7, total 101.3 wt%.) by EPMA. A compound showing the same XRD pattern was also obtained from a mixture of $BaSi_2$ and Si in a molar ratio of 1 : 4 by treatment under the same high-pressure and high-temperature condition. The XRD pattern was very similar to that of $EuGa_2Ge_4$ with space group *Cmcm* [11], and the structure was successfully determined in the same space group by Rietveld refinement (Fig. 2.). The refined structural parameters are summarized in Table 1. It was assumed that Ga and Ge atoms in $EuGa_2Ge_4$ are randomly distributed in the network. In $BaSi_6$ these sites are substituted by Si atoms. Geometry optimization of the structural parameters determined by the Rietveld refinements were performed using the *ab initio* program CASTEP [12], including the lattice constants and the coordinates. The results are compared in Table 1, together with the experimental data. Note the very good agreement between ex-

Table 1. Crystallographic data of $BaSi_6$ in comparison with the structural data optimized by CASTEP.

Lattice parameters, Å	Atom	Site	Atomic Coordinates and Isotropic Temperature Factors x	y	z	Beq, Å^2
Rietveld refinement						
S. G.: *Cmcm* (No. 63)	Ba	4*c*	0	0.273(4)	1/4	0.6(1)
$a = 4.485(1)$	Si1	8*f*	0	0.250(1)	0.537(1)	0.6(3)
$b = 10.375(2)$	Si2	8*f*	0	0.559(1)	0.351(1)	0.6(3)
$c = 11.969(3)$	Si3	8*f*	0	0.024(1)	0.599(1)	0.6(3)
Reliability factors (%)[a]: $Rwp = 5.33$, $Re = 1.95$, $Rp = 4.09$; goodness-of-fit $S(Rwp/Re) = 2.73$						
[a] *Rwp*, *R*-weighted pattern; *Re*, *R*-expected; *Rp*, *R*-pattern.						
CASTEP geometry optimization						
S. G.: *Cmcm* (No. 63)	Ba	4*c*	0	0.2787	1/4	
$a = 4.3999$	Si1	8*f*	0	0.2447	0.5384	
$b = 10.3113$	Si2	8*f*	0	0.5626	0.3518	
$c = 11.8842$	Si3	8*f*	0	0.0201	0.5977	

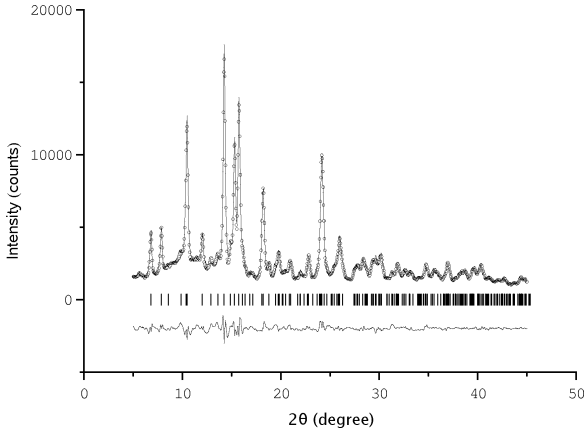

Fig. 2. Observed (open circle) and final calculated (line) profile plots, thick marks for Bragg peak positions, and difference profile plot from the Rietveld refinements of $BaSi_6$.

perimental data and the computationally determined parameters.

A schematic structural model of $BaSi_6$ is shown in Fig. 3, and selected bond lengths and angles are listed in Table 2. Each Ba atom is surrounded by 18 Si atoms forming an irregularly shaped polyhedral cage @Si_{18} as shown in Fig. 4a. The bond distances between the central Ba atom and the surrounding Si atoms are in a range of 3.2 – 3.58 Å, the average distance being 3.435 Å. In the type I clathrate Ba_8Si_{46}, the average bond distance Ba-Si in the Ba@Si_{20} cage is 3.365 Å, and that of the Ba@Si_{24} cage is 3.712 Å (Fig. 4b) [13]. The Ba@Si_{18} cage of $BaSi_6$ is as small as the Ba@Si_{20} cage of the Ba_8Si_{46} clathrate. The Ba@Si_{18} polyhedra are linked by sharing the faces so as to form tunnels along the *a* axis. All the Si atoms

Table 2. Selected bond lengths (Å) and angles (deg) in $BaSi_6$.

Ba-Si1	×2	3.444(12)	Si1-Si2		2.411(6)
Ba-Si1	×4	3.404(9)	Si1-Si2		2.393(15)
Ba-Si2	×2	3.202(11)	Si1-Si3		2.454(11)
Ba-Si2	×4	3.381(8)	Si2-Si2		2.418(16)
Ba-Si3	×2	3.579(7)	Si2-Si3		2.477(5)
Ba-Si3	×4	3.564(6)	Si3-Si3		2.424(16)
$Ba\text{-}Si_{ave}$		3.435			
Si1-Si1-Si1		136.9(5)	Si1-Si3-Si2	×2	113.9(4)
Si1-Si1-Si2	×2	101.9(4)	Si1-Si3-Si3		84.5(3)
Si1-Si1-Si3	×2	96.4(4)	Si2-Si3-Si2		129.7(4)
Si2-Si1-Si3		128.3(4)	Si2-Si3-Si3	×2	99.3(3)
Si1-Si2-Si2		124.1(5)			
Si1-Si2-Si3	×2	98.9(4)			
Si2-Si2-Si3	×2	103.9(4)			
Si3-Si2-Si3		129.7(4)			

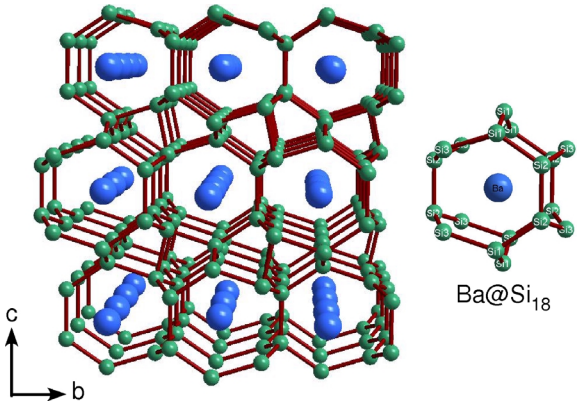

Fig. 3. Schematic illustration of the structure of $BaSi_6$. The Ba@Si_{18} polyhedra are linked by sharing faces to form tunnels running along the *a* axis.

are bonded to four different Si atoms in three different types of distorted tetrahedra (Table 2), forming a clathrate-like network containing Ba@Si_{18} polyhedral cages. $BaSi_6$ is isopointal with the clathrate structure of $EuGa_2Ge_4$.

The band structure was calculated with the program CASTEP, and the density of states (DOS) obtained is shown in Fig. 5. The non-zero DOS near the Fermi level shows that $BaSi_6$ is metallic. The electrical resistivity of $BaSi_6$ was measured by a conventional 4-probe method, and the result is shown in Fig. 6. The temperature dependence of the resistivity is almost flat over the temperature range from 300 to 2 K, although the resistivity of the order of ~ 0.1 Ωcm is not as small as that of metallic compounds. The relatively high electrical resistivity can be attributed to the many micro-cracks in the samples, which were observed under the scanning electron microscope for the EPMA measurement (Fig. 7).

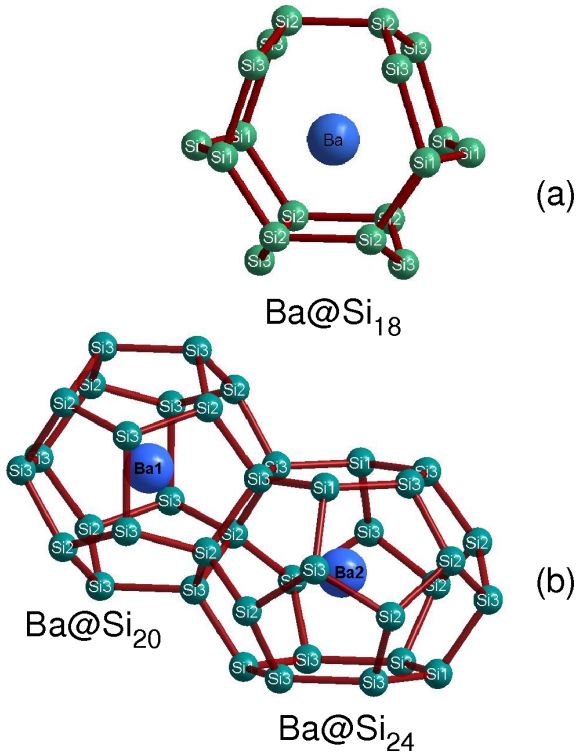

Fig. 4. Comparison of the polyhedra found in the clathrate structures, (a) $Ba@Si_{18}$ in $BaSi_6$ and (b) $Ba(1)@Si_{20}$ and $Ba(2)@Si_{24}$ in Ba_8Si_{46}. The average Ba-Si distances (d) are $d_{Ba-Si} = 3.435$, $d_{Ba1-Si} = 3.365$, and $d_{Ba2-Si} = 3.712$ Å.

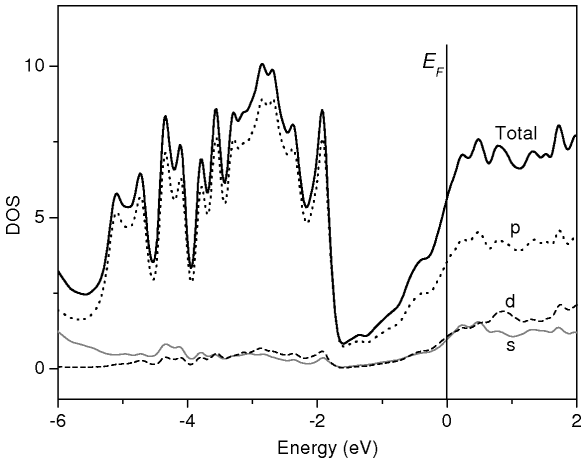

Fig. 5. Density of states (DOS) of $BaSi_6$; total DOS (solid line), and partial DOS for *s* (gray line), *p* (dotted line), and *d* (dashed line) orbitals.

It is obvious that the structures of the Ba-Si binary compounds are susceptible to compression at elevated

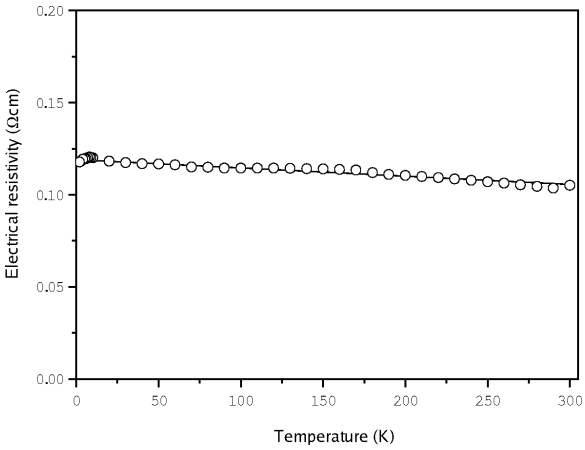

Fig. 6. Electrical conductivity of $BaSi_6$ as a function of temperature.

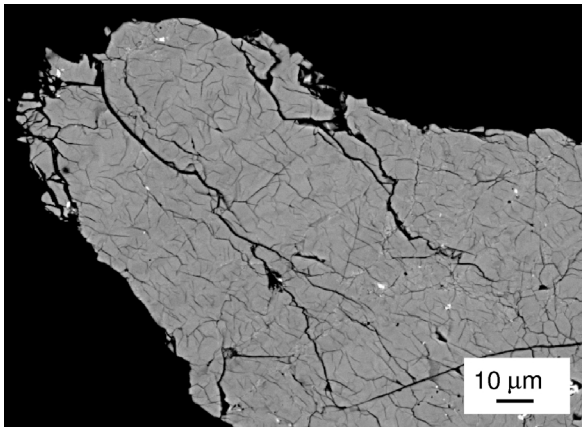

Fig. 7. Scanning electron micrograph of $BaSi_6$ showing a number of micro-cracks.

temperatures as shown in Fig. 1. Table 3 compares the volume changes between the reactant mixtures of $BaSi_2$ and Si and the products of different Si/Ba ratios. Note that there are large volume decreases in the formation of the Si-rich compounds; high-pressure and high-temperature synthesis is favorable for these compounds. It is also interesting to note that our recent study showed that the Ba_8Si_{46} clathrate compound has a slight deficiency at the Ba sites, and the composition was determined to be $Ba_{7.76}Si_{46}$ with a Si/Ba ratio of 5.93 [14], very close to the ratio in $BaSi_6$. The Ba_8Si_{46} clathrate with the Ba deficiency can be transformed into $BaSi_6$ without a compositional change.

A similar trend was also observed for Ge-rich compounds in the La-Ge and Sr-Ge systems under high-pressure and high-temperature conditions; new Ge-rich

Reactant mixture	Reaction conditions	Total volume (cm^3/mol)	Clathrate product	Clathrate volume (cm^3/mol)	Volume difference (%)
24 $BaSi_2$ + 52 Si	1.5 GPa, 800 °C	1884.7	$Ba_{24}Si_{100}$	1676.8	−9
8 $BaSi_2$ + 30 Si	3.0 GPa, 800 °C	778.2	Ba_8Si_{46}	663.6	−15
$BaSi_2$ + 4 Si	15 GPa, 1000 °C	100.2	$BaSi_6$	83.9	−16

Table 3. Comparison of molecular volumes between reactants and products.

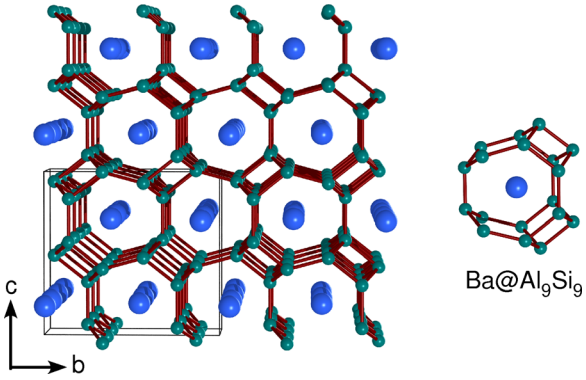

Fig. 8. Schematic illustration of the structure of the α-$BaAl_2Si_2$ and a Ba@(Al_9Si_9) polyhedral unit.

phases $LaGe_5$ [15] and $SrGe_{6-\delta}$ ($\delta \cong 0.5$) [16] were respectively obtained under high-pressure and high-temperature conditions of 5 GPa and 1200 °C. In the La-Ge system, La_3Ge, La_5Ge_3, La_4Ge_3, La_5Ge_4, LaGe, and $LaGe_2$ were prepared at ambient pressure. In the Sr-Ge system, Sr_2Ge, Sr_5Ge_3, SrGe, $Sr_{0.76}Ge$, $SrGe_2$ (trigonal), and $SrGe_2$ (orthorhombic) have been reported as yet. The new Ge-rich $SrGe_{6-\delta}$ phase is isotypic with $BaSi_6$. The DOS profile was calculated for $SrGe_{6-\delta}$ using the non-deficient germanide $SrGe_6$ [16], which is very similar to that shown for $BaSi_6$ in Fig. 5.

$EuGa_2Ge_4$, isotypic with $BaSi_6$, is a charge-balanced Zintl phase with a formal charge of $Eu^{2+}Ga^{-1}{}_2Ge^0{}_4$, and Ga^{-1} and Ge^0 can complete the clathrate covalent network with the octet configuration. It has been reported that $EuGa_2Ge_4$ is often associated with another charge-balanced Zintl phase, Type I clathrate $Eu_8Ga_{16}Ge_{30}$ [11]. If the Ga and Ge sites are denoted by E, the two charge-balanced Zintl phases have very close compositions, EuE_6 ($E/\mathrm{Eu} = 6$) and Eu_8E_{46} ($E/\mathrm{Eu} = 5.75$), respectively, and the formation conditions should be very similar. These two compounds were prepared from a mixture of the elements by direct heating at ambient pressure [11].

Fig. 8 shows the crystal structure of α-$BaAl_2Si_2$ which is isostructural with $BaAl_2Ge_2$ [17]. Note that the structure is composed of Ba@$(Al,Si)_{18}$ polyhedral cages very similar to Ba@Si_{18} of $BaSi_6$. Similar tunnels with Ba atoms are running along the a-axis formed by the sharing of faces of the polyhedra. α-$BaAl_2Si_2$ is a low-pressure polymorph, which is transformed into the high-pressure polymorph β-$BaAl_2Si_2$ having the $ThCr_2Si_2$ structure [17]. α-$BaAl_2Si_2$ is also a charge-balanced Zintl phase, and was prepared by simple direct heating of a mixture of the elements at ambient pressure.

More than 100 types of group IV clathrate compounds have been synthesized [18]. Most of them are charge-balanced Zintl compounds such as $Eu_8Ga_{16}Ge_{30}$ and $SrGa_{16}Ge_{30}$, and can be prepared from the mixtures of the elements by direct heating. A few exceptions are Ba_8Si_{46}, Na_8Si_{46}, and $(Na,Ba)_8Si_{46}$, where the clathrate covalent networks can be completed without using electrons from the guest metal atoms in the cages. The excess electrons from the guest metal atoms in the cages are accommodated in the antibonding orbital bands of the network. This type of compounds can be classified as "intercalation-type clathrate compounds" [19]. The intercalation-type clathrate compounds should be metallic, while the nature of the Zintl-type clathrate compounds is semiconducting. Most of the intercalation-type clathrate compounds cannot be prepared by direct heating under ambient pressure. Na_8Si_{46} [20] and $(Na,Ba)_8Si_{46}$ [21] were prepared by removing Na atoms *via* thermal decomposition of the Zintl compounds NaSi and $BaNa_2Si_4$, respectively. The binary intercalation-type clathrate compounds $Ba_{24}Si_{100}$, Ba_8Si_{46}, and $BaSi_6$ can be prepared only by using high-pressure and high-temperature conditions.

After the submission of this manuscript, another isotypic compound $EuSi_6$ and its ternary derivatives $EuSi_{6-x}Ga_x$ ($0 \leq x \leq 0.6$) have just been reported by Wosylus *et al.* [25]. These compounds were also prepared by applying a pressure of 8 GPa and a temperature of 1250 °C. There are a number of interesting similarities between the Eu and Ba analogues with regard to the structures and electrical properties. It has also been pointed out that the compounds with an excess of electrons can only be prepared by application of high pressure.

Conclusions

High-pressure and high-temperature synthesis favors the formation of Si-rich Ba-Si binary phases. The higher the pressure, the more Si-rich are the compounds formed. The new Si-rich compound $BaSi_6$ was prepared under a pressure of 15 GPa at 1000 °C. The structure was determined by Rietveld refinement, and the structural parameters were successfully reproduced by the geometry optimization using the *ab initio* program CASTEP. Similar trends were also found in Sr-Ge and La-Ge binary systems. $BaSi_6$ is a new type of clathrate compound, which can be classified into the intercalation type. Superconductivity could be anticipated as found in the other Si clathrates Ba_8Si_{46} and $Ba_{24}Si_{100}$, which become superconductors at $T_c = 8.0$ and 1.4 K, respectively.

Experimental

High-pressure and high-temperature experiments

$BaSi_2$ was prepared by an arc-melting method described elsewhere [6]. Ba_8Si_{46} was prepared from a stoichiometric mixture of $BaSi_2$ and Si powders by high-pressure treatment at 3 GPa and 800 °C using a cubic multianvil-type press [6]. High-pressure and high-temperature experiments were carried out using Kawai-type multianvils [22]. The samples were filled in a cylindrical *h*-BN cell with an inner diameter of 1.5 mm, which was surrounded by a thin Ta-tube heater. The heater was placed in a ZrO_2 tube, and the whole sample assembly was centred in a pierced CoO doped MgO octahedron with an edge length of 10 mm. The octahedron was placed in the center of eight truncated tungsten carbide cubes as anvils (truncation edge length: 4 mm) separated by pyrophyllite gaskets, and compressed in a multianvil apparatus up to 15 GPa, followed by heating to temperatures up to 1000 °C in 5 min. After keeping the sample at the temperature for one hour, it was cooled down to r. t. rapidly. Then the pressure was gradually released over the matrix.

Characterization

Powder X-ray diffraction patterns were measured on a diffractometer having a curved imaging plate (IP) detector (Rigaku-RAXIS) using graphite-monochromated MoK_α radiation ($\lambda = 0.71073$ Å). The radius of the IP was 127.4 mm, and the resolution was 0.044 deg/pixel. The powder sample was filled in a glass capillary with a diameter of 0.3 mm and rotated over 180 degrees on the ω axis. The intensity of the diffraction pattern measured by IP was traced along the horizontal line, and converted into the intensity *vs* diffraction angles (2θ) profile using the program package RAPID. The structure of $BaSi_6$ was analyzed on the profile data over the range from 5 to 45 deg using the software package TOPAS-Academic for the Rietveld analysis [23]. The composition was determined by an electron probe microanalyzer (JEOL JCMA-733II).

The geometry optimizations, the density of states, and band structure calculations were performed within the density functional theory (DFT) framework, using the program CASTEP [12, 24]. The calculations were performed using the GGA-PBE (generalized gradient approximation-Perduew-Burke-Ernezerhof) functional. Ultrasoft *pseudo* potentials were used within a plane wave basis with cutoff energy of 230 eV. A $6 \times 4 \times 4$ Monckhorst-Pack mesh was used for k-point sampling within the Brillouin zone. The structural parameters optimized included cell parameters and internal coordinates of atoms.

Acknowledgements

This study has been supported by a Grant-in-Aid for Scientific Research (No. 16205027 and 170380320) and the COE Research (No. 13E2002) of the Ministry of Education, Culture, Sports, Science, and Technology of Japan. The authors would like to thank Y. Shibata and H. Ishisako for their help in the EPMA analysis.

[1] J. Evers, J. Solid State Chem. **32**, 77 (1980).
[2] M. Imai, T. Hirano, Phys. Rev. B **58**, 11922 (1998).
[3] M. Imai, T. Kikegawa, Chem. Mater. **15**, 2543 (2003).
[4] H. Nakano, S. Yamanaka, J. Solid State Chem. **108**, 266 (1994).
[5] H. Fukuoka, K. Ueno, S. Yamanaka, J. Organomet. Chem. **611**, 543 (2000).
[6] S. Yamanaka, E. Enishi, H. Fukuoka, M. Yasukawa, Inorg. Chem. **39**, 56 (2000).
[7] S. Yamanaka, H. Kawaji, M. Ishikawa, in K. Sattler (ed.): Cluster Assembled Materials, Mater. Sci. Forum **232**, 103 (1996).
[8] T. Rachi, H. Yoshino, R. Kumashiro, M. Kitajima, K. Kobayashi, K. Yokogawa, K. Murata, N. Kimura, H. Aoki, H. Fukuoka, S. Yamanaka, H. Shimotani, T. Takenobu, Y. Iwasa, T. Sasaki, N. Kobayashi, Y. Miyazaki, K. Saito, F. Guo, K. Kobayashi, K. Osaka, K. Kato, M. Takata, K. Tanigaki, Phys. Rev. B **72**, 144504 (2005).
[9] A. San-Miguel, P. Melion, X. Blase, E. Reny, S. Yamanaka, J. P. Itié, Phys. Rev. B **65**, 054109 (2002).
[10] A. San-Miguel, P. Toulemonde, High Pressure Res. **25**, 159 (2005).

[11] W. Carrillo-Cabrera, S. Paschen, Y. Grin, J. Alloys Compd. **333**, 4 (2002).
[12] CASTEP is available from Accelrys, San Diego, CA, http://www.accelrys.com.
[13] H. Fukuoka, J. Kiyoto, S. Yamanaka, J. Solid State Chem. **175**, 237 (2003).
[14] H. Fukuoka, J. Kiyoto, S. Yamanaka, Inorg. Chem. **42**, 2933 (2003).
[15] H. Fukoka, S. Yamanaka, Phys. Rev. B **67**, 094501 (2003).
[16] H. Fukuoka, S. Yamanaka, E. Matsuoka, T. Takabatake, Inorg. Chem. **44**, 1460 (2005).
[17] S. Yamanaka, M. Kajiyama, S. N. Sivakumar, H. Fukuoka, High Pressure Res. **24**, 481 (2004).
[18] S. Bobev, S. Sevov, J. Solid State Chem. **153**, 92 (2000).
[19] M. Pouchard, C. Cros, P. Hagenmuller, E. Reny, A. Ammar, M. Ménétrier, J.-.M. Bassat, Solid State Sci. **4**, 723 (2002).
[20] J. S. Kasper, P. Hagenmuller, M. Pouchard, C. Cros, Science **150**, 1713 (1965).
[21] H. Kawaji, H. Horie, S. Yamanaka, M. Ishikawa, Phys. Rev. Lett. **74**, 1427 (1995).
[22] N. Kawai, S. Endo, Rev. Sci. Instrum. **41**, 1178 (1970).
[23] A. A. Coelho, TOPAS-Academic v1.0: General Profile and Structure Analysis Software for Powder Diffraction Data, Brisbane, 2004.
[24] M. D. Segall, P. J. D. Lindan, M. J. Probert, C. J. Pickard, P. J. Hasnip, S. J. Clark, M. C. Payne, J. Phys.: Condens. Matter **14**, 2717 (2002).
[25] A. Wosylus, Y. Prots, U. Burkhardt, W. Schnelle, U. Schwarz, Y. Grin, Solid State Sci. **8**, 773 (2006).